Attempts at an *in-situ* Raman study of Ceria / Zirconia catalysts in PM combustion

James A Sullivan,[1] Petrica Dulgheru[1,3], Idriss Atribak[2], Agustín Bueno-López[2], Avelina García-García,[2]

[1] *UCD School of Chemistry and Chemical Biology, Belfield, Dublin 4, Ireland.*

[2] *MCMA Group, Department of Inorganic Chemistry, University of Alicante, 03690, San Vicente, Alicante, Spain.*

[3] *Chemical Physics of Materials, Université Libre de Bruxelles, Campus de la Plaine, CP 243, B-1050 Bruxelles, Belgium*

Abstract.

$Ce_{(x)}Zr_{(1-x)}O_2$ catalysts with various Ce / Zr contents were studied using Raman spectroscopy under different gaseous atmospheres, at different temperatures and in the presence of a model soot. Catalysts with high concentrations of Zr fluoresced at elevated temperatures making analysis of their spectra impossible. This effect became even more pronounced at higher temperatures. CeO_2 and solid solutions with relatively low concentrations of Zr showed a red shift and a decrease in intensity of the characteristic F_{2g} peak at high temperatures under different atmospheres. The magnitude of the latter effect was higher under reducing atmospheres. These changes are reversible upon cooling, showing that they relate to a lattice expansion effect rather than any major chemical change to the material. In the presence of the model soot the Raman spectra of all materials was much decreased due to the absorption of the incident and scattered radiation by the soot particles. The presence of soot does not change the relative intensities or positions of the peaks in the spectra of the solid solutions. Evidence is shown for the production of a Ce^{3+}-CO species following interaction between the soot and the surface at high temperature in an inert atmosphere.

Keywords: $Ce_xZr_{1-x}O_2$, PM combustion, *in-situ* Raman Spectroscopy,

Introduction

Because of the detrimental effects on human health as well as the global and local environment the remediation of Particulate Matter (PM) formed in diesel and gasoline combustion chambers is an area of considerable research activity both within our group and worldwide [1-10]. The use of catalysts to promote the oxidation of PM has resulted in much research in technologies such as the diesel particulate filter (DPF) [3-4] and the diesel particulate NO_x reduction systems (DPNR) [9-10].

The use of Ceria-Zirconia solid solutions, where Zr ions are incorporated into the fluorite CeO_2 structure, in promoting this reaction has been discussed by several authors [11-15]. The rationale behind the use of these materials in this reaction is related to the oxygen storage capacity of the catalysts. CeO_2 can desorb and re-adsorb O_2 through formation and consumption of a Ce_2O_3 oxide

[16-20]. The oxygen atoms involved in this process are active for promotion of various combustion and reforming reactions [21-25] and for this reason (as well as their ability to dampen excursions to overly fuel rich or fuel lean exhaust conditions) $Ce_{(x)}Zr_{(1-x)}O_2$ catalysts are used as supports in many catalytic formulations.

The characterization of $Ce_{(x)}Zr_{(1-x)}O_2$ solid solutions by Raman spectroscopy has been widespread [26-30]. The structure of CeO_2 is face centered cubic (fluorite type). It can be described as 8 O^{2-} ions linked together by the edges, with the cerium ion at the centre of the oxygen cube. One of the triply degenerate F_{2g} modes (~ 465 cm^{-1}) can be viewed as a symmetric breathing vibrational mode of the O ions around each cation [26, 27]. This mode is, therefore, very sensitive to the oxygen sub-lattice disorder resulting from exposure to reducing / oxidising atmospheres. Furthermore, Raman spectroscopy has been used to monitor the formation of a Ce^{3+} species (in the presence of CO) following reduction of a portion of CeO_2 [31 – 32].

The soot combustion activity and the room temperature Raman spectra of the materials we discuss here have previously been reported [33]. It has been shown that all these materials promote soot oxidation in air and NO / O_2 (when reactivity profiles are compared to those of non-catalysed soot oxidations). The activity of the catalysts is inversely related to the Zr concentration. The room temperature Raman spectra of these materials has also previously been reported and it has been found that the F_{2g} peak shows a decrease in intensity and a change in position (towards higher energy) as the ZrO_2 content within the solid solution is increased. This decrease is related to a change in the crystal structure which accompanies the decrease in the [Ce] (since this peak is related to a breathing mode of O^{2-} ions in the fluorite lattice).

In this work we describe the Raman spectra of a series of ceria zirconia mixed oxides in contact with a model Particulate Matter (Printex U [34]) under several gaseous atmospheres and following treatment at different temperatures. To our knowledge there have been no reports of a Raman spectroscopic study of the interaction between $Ce_{(x)}Zr_{(1-x)}O_2$ mixed oxides and PM as a function of the gaseous atmosphere or the reaction temperature.

Experimental

Catalyst synthesis and Catalyst : Soot mixture preparation

CeO_2, ZrO_2 and mixed oxide ($Ce_xZr_{1-x}O_2$) catalysts were prepared using a co-precipitation technique [33]. The catalysts were mixed in defined ratios (50 catalyst: 1 soot) with a model soot (Printex-U) to approximate a loose contact situation.

Raman Spectroscopy

Raman spectra were recorded using a Senterra III Raman Scope (Bruker) equipped with a Unilab II (Bruker) fibre optic probe. A diode laser (λ = 785 nm) operated at 25 mW was used as Raman excitation source and a germanium thermoelectrically cooled Charged Couple Device (Andorf) as detector. This probed the catalyst or catalyst soot mixture, (~200 mg) which was held in a CCR 1000 high temperature catalytic cell (Linkam). Use of the cell allowed control of the temperature and the gaseous atmosphere surrounding of the catalyst.

Thermogravimetric Analysis

TGA was carried out using a Q500 TGA (TA Instruments) thermogravimetric balance equipped with an Evolved Gas Analysis furnace. The EGA furnace was fitted with an exhaust port which allowed coupling of the TGA to a Quadrupole MS (HPR20, Hiden). This tandem TGA-MS system was able to monitor both the mass loss (as % mass loss, or derivative weight change profiles) and the composition of desorbed gases simultaneously. The catalyst soot mixtures were held in a flow of air (90 mL min^{-1}) and the temperature was ramped at a rate of 10 °C min^{-1})

Results and Discussion

Soot combustion activity and room temperature Raman spectra

The activity of these materials in promoting soot combustion (as measured using TGA rather than a fixed bed reactor) and their room temperature Raman spectra are essentially the same to those reported previously [33]. These are shown in the supporting information as Figure S1 and Figure S2.

Figure 1 shows the Raman spectra (200 – 2000 cm^{-1}) of the entire range of materials studied. Features in the Raman spectra of the materials between 1000 cm^{-1} and 2000 cm^{-1} have been ascribed to surface formats and carbonates [35-36]. These peaks become less pronounced as the ZrO_2 content increases.

The Raman spectra at energies around that of the F_{2g} peak (between 200 cm^{-1} and 650 cm^{-1}) also show evidence for the presence of defects once Zr is introduced into the lattice. These are shown in the inset of Figure 1 (a) where the spectra of the CeO_2 and $Ce_{0.8}Zr_{0.2}O_2$ materials are displayed. This has also been previously reported [26-27]. Relevant assignments of Zr-rich samples were also reported elsewhere [33].

Effect of temperature and gaseous atmosphere on the F_{2g} peak of CeO_2.

Figure 2 shows the F_{2g} peak of the CeO_2 sample recorded at room temperature, at 500 °C and again at room temperature under both a reducing H_2 atmosphere and an oxidizing O_2 atmosphere. Recall that this vibration relates to the symmetrical breathing mode of the O ions around the cation and its position and intensity are sensitive to the O concentration of the material.

The F_{2g} peak of the sample held at room temperature in H_2 is slightly more intense than that in the equivalent spectrum recorded in O_2. It is clear that upon heating the material the F_{2g} peak is shifted to lower energies (from ~460 cm^{-1} to ~450 cm^{-1}) and its intensity is decreased. The latter effect is far more pronounced in the presence of H_2 than in an oxidizing atmosphere.

Upon re-cooling to room temperature the positions of the peaks returns to ~460 cm^{-1} and their intensity increases once more. The peak relating to the sample treated in O_2 is slightly more intense following the temperature cycle than it had been initially while the reverse is true of the sample which had been treated in H_2, *i.e.* the F_{2g} peak is slightly less intense following the high temperature reduction than it had been initially.

The fact that the sample under O_2 at RT shows a less intense peak than the same sample under H_2 is puzzling. Taken at face value, this suggests that the addition of H_2 has increased the concentration of the cubic species responsible for the vibration, while the addition of O_2 has decreased this concentration. This is plainly not reasonable.

Therefore, we suggest that these relatively small intensity changes (and those noted once the materials are re-cooled following heat treatments) are within the error limits of the technique. In these experiments spectral intensity depends significantly on aspects such as the positioning of the fiber optic probe and homogeneity of the sample. Relatively small changes such as these can easily be explained by these experimental artefacts. However, the intensity changes noted upon heating (especially in the presence of H_2) are far greater.

The individual sets of spectra showing the progression of this peak as a function of temperature in both O_2 and H_2 are shown in the supporting information (see figures S3 and S4).

The decreases in intensity at higher temperatures, coupled with the shift in the peak maxima under these conditions are important. The fact that these are, for the most part, reversible once the temperature is cooled back to room temperature suggest that they do not relate to any major chemical change taking place within the material and rather the changes are due to the thermal expansion of the fluorite lattice at 500 °C. Similar reversible effects have been noted previously with a $Ce_{0.7}Pr_{0.3}O_2$ sample [37] and with a range of CeO_{2-y} sub oxides [38]. They have also been noted in V_2O_5 systems [39] and have been explained by Bell and Iglesia [40]. Their explanation of these phenomena related to thermal expansion (peak position) and changes in the populations of vibrational energy levels (peak intensity / broadening) with increasing temperature.

Bell also points out that this affects the use of Raman spectroscopy for *in-situ* or *operando* techniques [41]. These results confirm that the position and intensity of these Raman peaks change as a function of temperature. This makes the observation of these peaks under different reaction conditions, and subsequent correlation of their behavior with any reactivity, *i.e. operando* spectroscopy, fraught.

Effect of ZrO_2 content on Raman spectra at higher temperature

The presence of Zr has a further effect on the Raman spectra of the materials once the temperature is raised substantially above room temperature. In samples containing high concentrations of

Zirconia there is a large fluorescence peak seen at higher temperatures. The intensity of this fluorescence increases as a function of both [ZrO_2] and T.

While it is possible that the use of a different excitation laser wavelength (from the 785 nm used in the current study) might ameliorate this effect unfortunately using our system it was not possible to determine whether this was the case. DRS spectroscopy has shown no absorbance by the materials at this wavelength. A certain amount of fluorescence (at lower T and lower [ZrO_2]) can be corrected for using the Concave Rubber band treatment. Figure S5 shows this effect.

The two sets of data shown in figures 2 and discussed above (in which firstly temperature was shown to affect the position and intensity of the diagnostic F_{2g} peak and secondly increased ZrO_2 content leads to fluorescence at higher temperatures) informed the future collection of spectra. Specifically, these outcomes have lead us to (a) collect spectra at room temperature following treatments in the isolated cell at higher temperatures and (b) concentrate our studies on samples containing lower ZrO_2 content.

Effect of PM on Raman spectrum

Figure 3 shows the Raman spectrum of Printex-U. Two broad vibrations can be observed: a very strong Raman vibration in the 1190 cm^{-1} – 1472 cm^{-1} region centred at 1330 cm^{-1}, and another broad vibration mode in the 1600 cm^{-1} – 1963 cm^{-1} region centred at 1695 cm^{-1}. The spectrum also shows a small peak in the 1472 cm^{-1} – 1600 cm^{-1} region with a maximum appearing at 1550 cm^{-1}.

Sadezky *et al.* [42] have recorded the Raman spectra of pure graphite and observed a very strong band at 1550 cm^{-1} (the G band) and have attributed it to a pure graphite lattice vibration with E_{2g} symmetry. A less intense band at 1360 cm^{-1} (referred to as the D1 band) has been ascribed to defects in the graphite lattice. Another weak band (the D2 band) has been observed in pure graphite at 1620 cm^{-1} (and was also ascribed to defects in the graphite lattice).

Other workers [43-47] have studied different types of synthetic carbonaceous PM and graphitic materials and concluded that the Raman spectra of carbonaceous particulate matter can be interpreted in terms of highly disordered graphitic structures. According to these researchers a band at approximately 1360 cm^{-1} is very specific for disordered carbon samples (the transition is forbidden in pure graphite) and a vibration appearing at approximately 1580 cm^{-1} can be attributed to an ideal graphite lattice vibration with E_{2g} symmetry.

Printex-U displays all these vibration modes in the 1000 cm^{-1} – 1800 cm^{-1} region making the deconvolution between surface carbonate species, which are always present on these oxide surfaces (see Figure 1) in the presence of CO_2, and Printex-U very difficult (see above).

Figure 4 compares the Raman spectra of Printex-U with those of CeO_2 and a CeO_2 / Printex-U mixture. The mixed sample was black, in contrast with the light yellow CeO_2. In Figure 4, in order to scale the spectra onto one plot, the spectrum for CeO_2 was reduced by a factor of 25 while that for Printex-U was reduced by a factor of 5. This scaling is required because the intensity of the Raman signal is very much decreased in the presence of PM. The addition of relatively small (2% of the mixture by mass) amounts of soot has a dramatic effect on the intensities of the spectra collected, *i.e.* the Raman Effect is much decreased in presence of Printex-U.

According to Li *et al.*[48], when the excitation laser and scattered light are strongly absorbed by the sample, smaller amounts of scattered light escapes and therefore the observed Raman signal is weakened. This effect can be further seen in Figure 6 where the Raman spectra of two of the samples in the presence and absence of PM are shown. The Raman spectrum in the presence of PM is considerably weaker than when the pure sample is analysed.

The spectra of the oxide – soot samples also lack features relating to the G and D bands of the PM (see above). It should be noted that these samples are mixtures in which the PM concentration is diluted by a factor of 50 compared to the pure Printex U sample shown in Figure 3.

The fact that clear bands relating to Printex-U are not observable at these low concentrations, coupled with the fact that increasing the Printex-U concentration in the mixture further quenches the Raman spectra of the oxides of interest adds a further difficulty to attempts to observe soot combustion *in-situ* using Raman spectroscopy. However, the removal of soot through oxidation can be followed indirectly using this effect (see below).

Apart from the aforementioned decrease in Raman intensity associated with the absorption of laser and scattered light by the PM, almost no differences can be observed when comparing the Raman spectra shown in Figure 5. The overall decrease in intensity applies to the entire spectrum. This makes less intense peaks appear significantly smaller and the smaller peaks seem to disappear. These weaker peaks are removed but the position and relative intensities of the major carbonate related peaks and the F_{2g} peak remains the same in the presence and absence of soot – suggesting there is no redox reaction interaction between the two components which leads to an observable (using Raman spectroscopy) removal of oxygen from the fluorite phase.

Raman Spectra confirming PM oxidation.

Figure 6 shows the effect on the intensity of the Raman spectra of treating a $Ce_{0.8}Zr_{0.2}O_2$ / Printex-U mixture in an oxidizing environment (NO / O_2) at elevated temperatures. Because of the fluorescence problems at higher temperatures (see Figure S5) these spectra are recorded at room temperature before and after the high temperature treatment. It is clear that, while the relative intensities and positions of the individual peaks in each spectrum are unchanged following the treatment, the overall intensity of the spectra is significantly increased following the excursion to higher temperatures in NO / O_2. It should be noted that the final intensity is still approximately 8 times lower than it had been in the absence of PM (Figure 5). We ascribe the increase in intensity to the oxidation of PM at the temperatures of the NO / O_2 treatment and the subsequent lessening of the quenching effects seen above, *i.e.* there is less PM in the system to absorb the incident and scattered radiation.

Formation of Ce^{3+} – CO species from reaction between $Ce_xZr_{1-x}O_2$ and PM

Figure 7(a) shows the TGA profile of a sample of $Ce_{0.8}Zr_{0.2}O_2$ – PM mixture which was held in a He flow at 500 °C for 250 min. The mass spectrometer profiles for O_2 (m / e = 32) and CO_2 (m / e = 44) evolved during the experiment are also shown. During the 250 min. of the experiment approximately 1.6% of the mass of the mixture was lost. This mass loss was accompanied by the removal of CO_2 and O_2 from the system. The CO_2 profile shows maximum production of CO_2 at the beginning of the experiment followed by an exponential decrease. This was mirrored by the production of O_2 which began at a relatively low level and subsequently increased throughout the course of the experiment.

These observations can be explained as being due to desorption of O_2 from the ceria containing materials (and the concomitant formation of Ce^{3+}) [16-23]. Initially this O_2 (rather than leaving the system) reacted with the PM and formed CO_2. As the concentration of proximate PM in the system decreased the volumes of CO_2 produced decreased and the amount of O_2 leaving the system un-reacted increased.

Figure 7(b) shows a series of normalized Raman spectra (where they were normalized using the intensity of the F_{2g} peak (see Figure S6)) showing essentially the same experiment. The spectra show a $Ce_{0.8}Zr_{0.2}O_2$ catalyst admixed with soot, the same sample following a 4 h treatment in He and again following a 30 h treatment in He. In Figure 7(b) the development of a peak at approximately 2100 cm^{-1} is clearly visible. This peak is not present in oxidized $Ce_{0.8}Zr_{0.2}O_2$. Peaks in this spectral region have previously been noted by several authors [31-32, 49-50] and are specific to reduced CeO_2 samples. Swanson and co-workers have assigned the species as a Ce^{3+} – CO vibration. This suggests that either atomic oxygen on the surface of the $Ce_{0.8}Zr_{0.2}O_2$ catalyst reacted with PM, or that a desorbed O_2 reacted with PM to form CO or CO_2 which subsequently adsorbed on the formed Ce^{3+} sites. The re-adsorption of carbon-containing gaseous products on the catalyst leads to the exchange

of oxygen between the adsorbed gases and the catalyst, as previously demonstrated [51]. The Ce^{3+}-CO species observed by Raman spectroscopy may be reaction intermediates of these oxygen exchange processes.

In either case this appears to be evidence for the reaction between the $Ce_{0.8}Zr_{0.2}O_2$ catalyst and the PM under inert gas conditions. This conclusion is consistent with previous studies of the ceria-catalysed soot combustion mechanism carried out using isotopically labeled oxygen in a TAP reactor [52]. It was concluded that the driving force for the pure ceria-catalysed soot combustion is O_2 uptake by ceria, which destabilizes surface oxygen entities delivering active oxygen species from the ceria to soot. On the contrary, in La^{3+}-doped ceria catalysts (which have improved redox properties relative to ceria), the oxygen in the lattice itself oxidizes soot and subsequently gas phase oxygen fills the lattice vacancies.

On the other hand changes in the shape and position of the F_{2g} peak following these treatments are not seen (see figure S6). If significant proportions of the Ce^{4+} content of the material had been reduced to Ce^{3+} (through loss of O_2 from the fluorite lattice) we might have expected this peak to shift (as was the case in Figure S2).

Conclusions

Collecting Raman spectra from these mixed oxides in the presence of PM under reaction conditions is complicated by several effects.

Firstly, under conditions where the samples are irradiated with a 785 nm laser, the Zr-containing materials fluoresce at high temperatures. The extent of this fluorescence is correlated with the concentration of ZrO_2 within the materials. Secondly, in the absence of soot at high temperature there is also a change in the position and intensity of the characteristic F_{2g} band. This change involves a movement of the peak to lower energies (due to thermal expansion of the absorbing particle) and a decrease in the peak intensity (related to a broadening of the peak due to the occupancy of significant numbers of vibrational sub-levels at these temperatures). These changes were more pronounced when the gaseous atmosphere was reducing (H_2) but were also present when the atmosphere was oxidizing (O_2). These peak shifts were reversible upon cooling the samples in the reactive atmospheres.

Thirdly, the Raman Effect is much decreased in the presence of soot due to the absorption of both the incident laser light and the scattered signal. This results in far less intense spectra in the presence of soot and also in a changing spectral intensity during reaction as soot was removed from the *in-situ* cell.

Finally, the production of surface carbonates as a result of soot combustion is masked by the bands due to the soot itself and it is not possible to de-convolute these signals.

These observations led us to collect all subsequent spectra at room temperature following whatever treatments (temperature / gaseous environment) the catalysts (or catalyst soot mixtures) were subjected to.

A $Ce_{0.8}Zr_{0.2}O_2$ catalyst in contact with Printex-U developed Raman bands relating to a Ce^{3+}–CO species following an extended treatment in inert gas at 500 °C. This suggests that the catalyst material was able to transfer an O atom from the catalyst surface to the soot, forming CO or CO_2, portions of which subsequently adsorbed onto the reduced catalyst.

Acknowledgements

We would like to acknowledge EPA Ireland for the provision of a studentship for PD.

References

[1] Dobbins, R. A., Fletcher, R. A. and Chang, H.-C. Combustion and Flame, 115, (1998), 285-298.

[2] J.Hansen, and L.Nazarenko, Proc. Natl. Acad. Sci., 2004, 101, 423-428

[3] U. Hoffmann, T. Rieckmann and J. X. Ma, Chemical Engineering Science 1991, 46, 1101-1113.

[4] B. C. Choi, Y. B. Yoon, H. Y. Kang and M. T. Lim, International Journal of Automotive Technology 2006, 7, 527-534.

[5] J.A. Sullivan and P. Dulgheru. Applied Catalysis B: Environmental, (2010), 99, 235-241.

[6] J.A. Sullivan, O. Keane O and L. Maguire, Catal. Comm. 6, (2005), 472-475.

[7] J.A. Sullivan and O. Keane Catal. Today, 114, (2006), 340-345.

[8] J.A. Sullivan, O. Keane, A. Cassidy, Applied Catalysis B: Environmental 75, (2007), 102-106

[9] L. Castoldi, N. Artioli, R. Matarrese, L. Lietti, P. Forzatti. Catalysis Today, 157, 1-4, (2010) 384-389.

[10] R. Matarrese, L. Castoldi, L. Lietti, P. Forzatti. Topics in Catalysis, 52, 13-20, (2009), 2041-2046.

[11] C. K. Loong and M. Ozawa, Journal of Alloys and Compounds 2000, 303, 60-65.

[12] Y. C. Hu, P. Yin, T. Liang, W. Jiang and B. Liu, Journal of Rare Earths 2006, 24, 86-89.

[13] J. R. Gonzalez-Velasco, M. A. Gutierrez-Ortiz, J. L. Marc, M. P. Gonzalez-Marcos and G. Blanchard, Applied Catalysis B-Environmental 2001, 33, 303-314.

[14] R. Craciun, W. Daniell and H. Knozinger, Applied Catalysis A: General 2002, 230, 153-168.

[15] P. Fornasiero, J. Kaspar, T. Montini, M. Graziani, V. Dal Santo, R. Psaro and S. Recchia, Journal of Molecular Catalysis A-Chemical 2003, 204, 683-691.

[16] Q. Fu, S. Kudriavtseva, H. Saltsburg and M. Flytzani-Stephanopoulos, Chemical Engineering Journal 2003, 93, 41-53.

[17] L. Yang, O. Kresnawahjuesa, R.J. Gorte, Catalysis Letters, 72, 1-2, (2001) 33-37.

[18] S.J. Schmieg, D.N. Belton, Applied Catalysis B Environmental, 6, 2, (1995), 127-144

[19] K. Krishna, A. Bueno-Lopez, M. Makkee and J. A. Moulijn, Applied Catalysis B-Environmental 2007, 75, 210-220.

[20] P. Fornasiero, G. Balducci, R. DiMonte, J. Kaspar, V. Sergo, G. Gubitosa, A. Ferrero and M. Graziani, Journal of Catalysis 1996, 164, 173-183.

[21] A. Bueno - Lopez, K. Krishna, M. Makkee and J. Moulijn, Catalysis Letters 2005, 99, 203-205.

[22] F.D. Silva, J.A.C. Ruiz, K.R. de Souza, J.M.C. Bueno L.V. Mattos, F.B. Noronha, C.E. Hori. Applied Catalysis A: General, 364, 1-2, (2009), 122-129.

[23] S.M. de Lima, I.O. da Cruz, G. Jacobs, B.H. Davis, L.V. Mattos, F.B. Noronha, Journal of Catalysis, 257, 2, (2008), 356-368.

[24] A. Martorana, G. Deganello, A. Longo, A. Prestianni, L. Liotta, A. Macaluso, G. Pantaleo, A. Balerna, S. Mobillo. Journal of Solid State Chemistry, 177, 4-5, (2004), 1268-1275.

[25] J.R. Gonzalez-Velasco, M.A. Gutierrez-Ortiz, J.L. Marc, M.P. Gonzalez-Marcos, G. Blanchard. Applied Catalysis B: Environmental, 33, 4, (2001) 303-314.

[26] M. Fernandez-Garcia, A. Martinez-Arias, A. Iglesias-Juez, C. Belver, A. B. Hungria, J. C. Conesa and J. Soria, Journal of Catalysis 2000, 194, 385-392.

[27] A. Trovarelli, Catalysis Reviews-Science and Engineering 1996, 38, 439-520.

[28] A. Trovarelli, G. Dolcetti, C. Deleitenburg, J. Kaspar, P. Finetti and A. Santoni, Journal of the Chemical Society-Faraday Transactions 1992, 88, 1311-1319.

[29] P. Fornasiero, N. Hickey, J. Kaspar, T. Montini and M. Graziani, Journal of Catalysis 2000, 189, 339-348.

[30] P. Fornasiero, J. Kaspar and M. Graziani, Applied Catalysis B-Environmental 1999, 22, L11-L14.Characterisation by Raman

[31] C. Binet, A. Badri and J. C. Lavalley, Journal of Physical Chemistry 1994, 98, 6392-6398.

[32] A. Bensalem, F. Bozonverduraz and V. Perrichon, Journal of the Chemical Society-Faraday Transactions 1995, 91, 2185-2189.

[33] I. Atribak, B. Azambre, A. Bueno Lopez, A. Garcia-Garcia. Applied Catalysis B Environmental, 92, 1-2, (2009), 126-137.

[35] J. Kaspar, P. Fornasiero, G. Baiducci, R. Di Monte, N. Hickey and V. Sergo, Inorganica Chimica Acta 2003, 349, 217-226..

[36] P. Fornasiero, J. Kaspar and M. Graziani, Journal of Catalysis 1997, 167, 576-580.

[37] S. Rossignol, F. Gerard, D. Mesnard, C. Kappenstein and D. Duprez, Journal of Materials Chemistry 2003, 13, 3017-3020.

[38] J.E. Spanier, R.D. Robinson, F.Zhang, S.W. Chan, I.P. Herman, Physical Review B, 2001, 64, 245407.

[39] I.E. Wachs, S.S. Chan, Applied Surface Science, 1984, 20, 181

[40] S Xie, E. Iglesia, A.T.Bell, Langmuir, 2000, 16, 7162

[41] S Xie, E. Iglesia, A.T.Bell, J. Phys. Chem B, 2001, 105, 5144 - 5152

[42] A. Sadezky, H. Muckenhuber, H. Grothe, R. Niessner and U. Poschl, Carbon 2005, 43, 1731-1742.

[43] A. Cuesta, P. Dhamelincourt, J. Laureyns, A. Martinezalonso and J. M. D. Tascon, Carbon 1994, 32, 1523-1532.

[44] A. Cuesta, P. Dhamelincourt, J. Laureyns, A. Martinez-Alonso and J. M. D. Tascon, Journal of Materials Chemistry 1998, 8, 2875-2879.

[45] A. Cuesta, P. Dhamelincourt, J. Laureyns, A. Martinez-Alonso and J. M. D. Tascon, Applied Spectroscopy 1998, 52, 356-360.

[46] R. Escribano, J.J. Sloan, N. Siddique, N. Sze, T. Dudev, Vibrational Spectroscopy, 26, 2, (2001) 179-186.

[47] T. Jawhari, A. Roid and J. Casado, Carbon 1995, 33, 1561-1565.

[48] K. Z. Li, H. Wang, Y. G. Wei and D. X. Yan, Journal of Physical Chemistry C 2009, 113, 15288-15297.

[49] M. Swanson, V. V. Pushkarev, V. I. Kovalchuk and J. L. d'Itri, Catalysis Letters 2007, 116, 41-45.

[50] G. S. Nolas, V. G. Tsoukala, S. K. Gayen and G. A. Slack, Optics Letters 1994, 19, 1574-1576.

[51] A. Bueno-López, K. Krishna, M. Makkee. Appl. Catal. A 2008, 342, 144–149.

[52] A. Bueno-López, K. Krishna, B. van der Linden, G. Mul, J.A. Moulijn, M. Makkee. Catal. Today 2007, 121, 237–245.

Figure 1

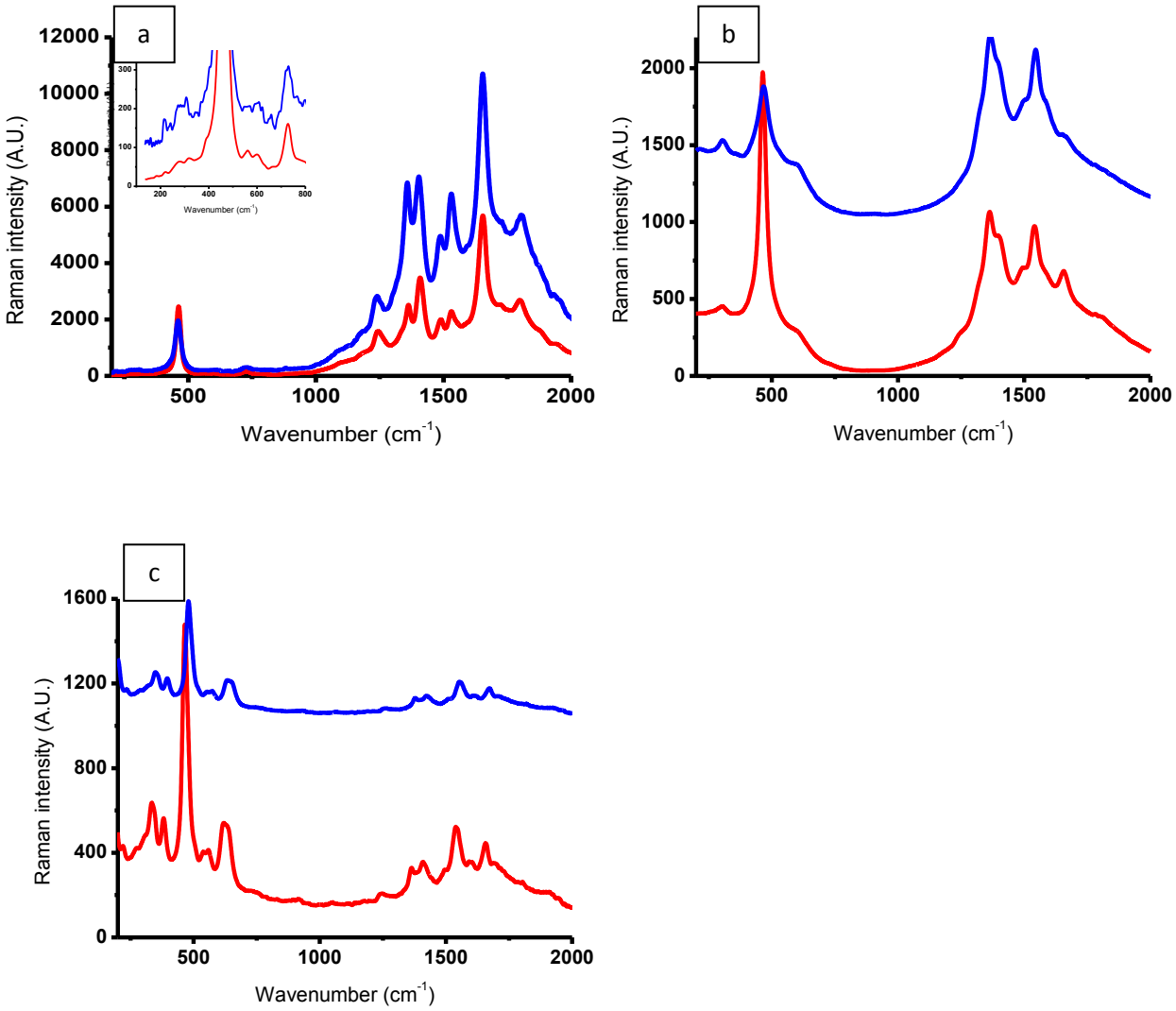

Figure 1. The 200-2000 cm^{-1} region of the Raman spectra of $Ce_xZr_{(1-x)}O_2$. Plot (a) compares the spectra of CeO_2 (lower) and $Ce_{0.8}Zr_{0.2}O_2$ (upper), plot (b) compares the spectra of $Ce_{0.6}Zr_{0.4}O_2$ (lower) and $Ce_{0.4}Zr_{0.6}O_2$ (upper) and plot (c) compares the spectra of $Ce_{0.2}Zr_{0.8}O_2$ (lower) and ZrO_2 (upper). The inset of plot (a) shows the region around the F_{2g} peak)

Figure 2

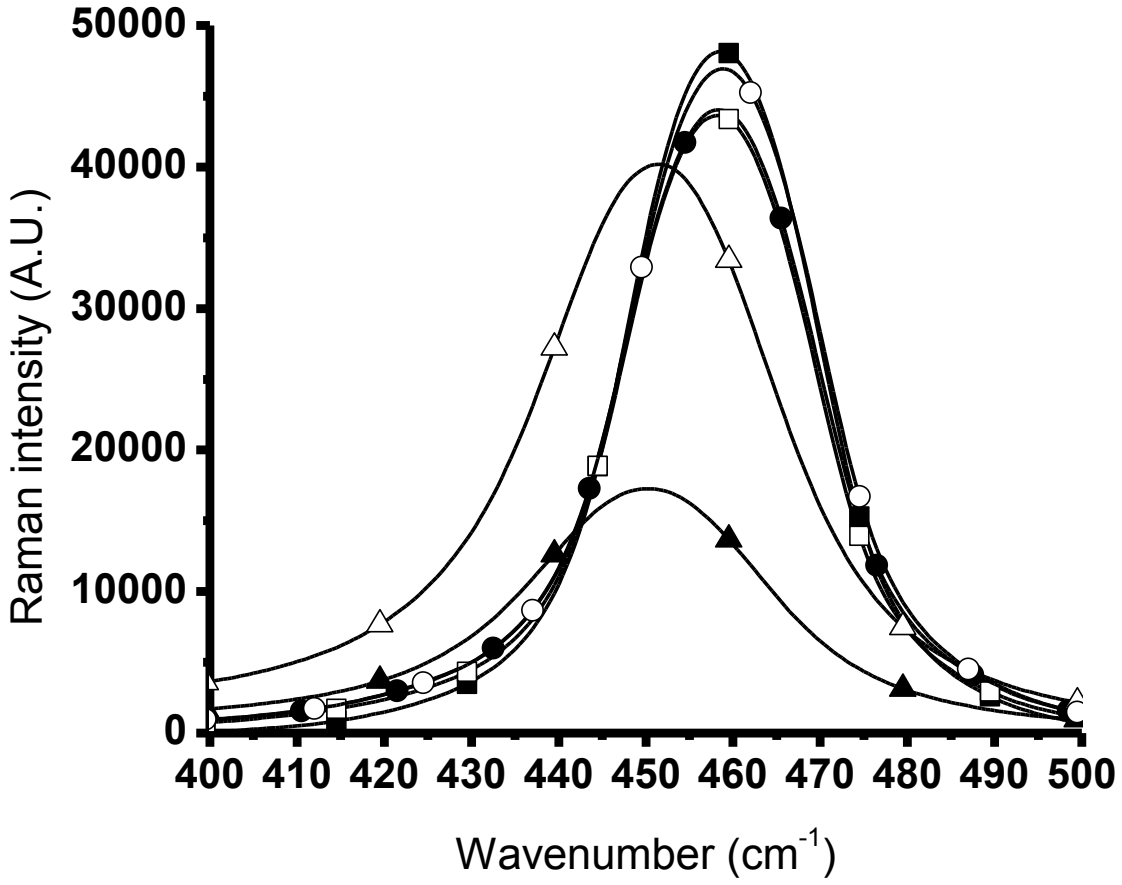

Figure 2. F_{2g} peak of CeO_2 recorded at room temperature (□,■), at 500 °C (△, ▲) and again at room temperature (❍, ●) in a H_2 atmosphere (filled symbols) and an O_2 atmosphere (empty symbols). Spectra have been corrected for fluorescence using the Concave Rubber Band function.

Figure 3

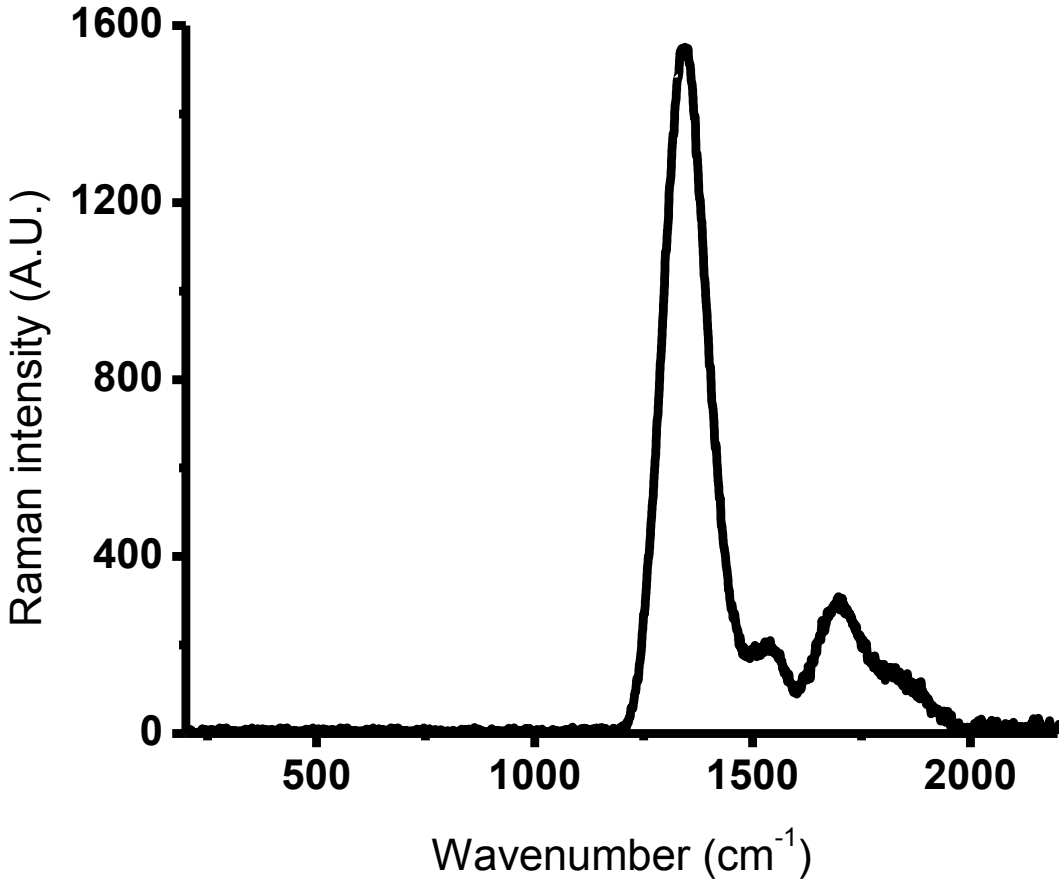

Figure 3. Raman spectrum of Printex U, a model soot.

Figure 4

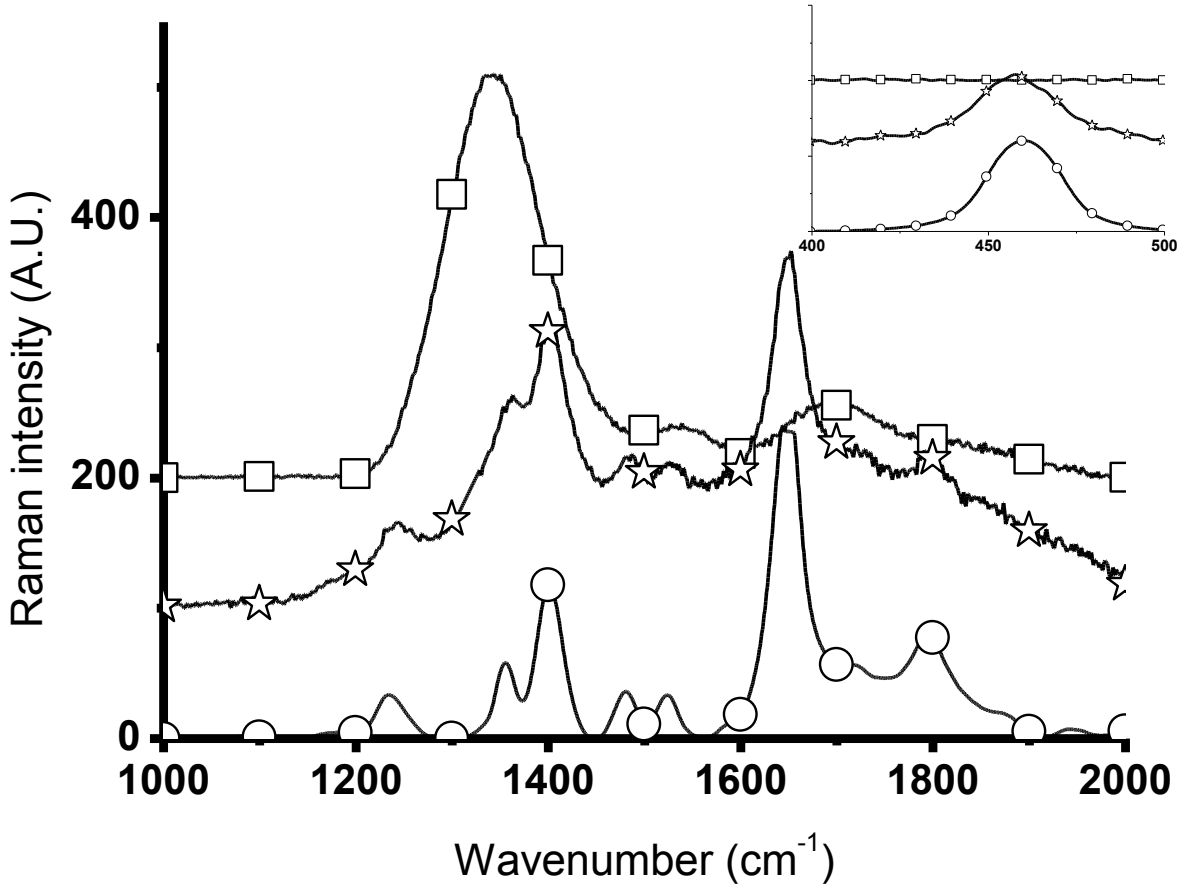

Figure 4. The 1000 cm^{-1} – 2000 cm^{-1} region of the Raman spectra of CeO_2 (○),.CeO_2-U (☆) and Printex U (□),Inset shows the 400 – 500 cm^{-1} region (F_{2g} peak) from the same spectra. For clarity, profiles were displaced and the CeO_2 and Printex U spectra were reduced by factors of 25 and 5 respectively.

Figure 5

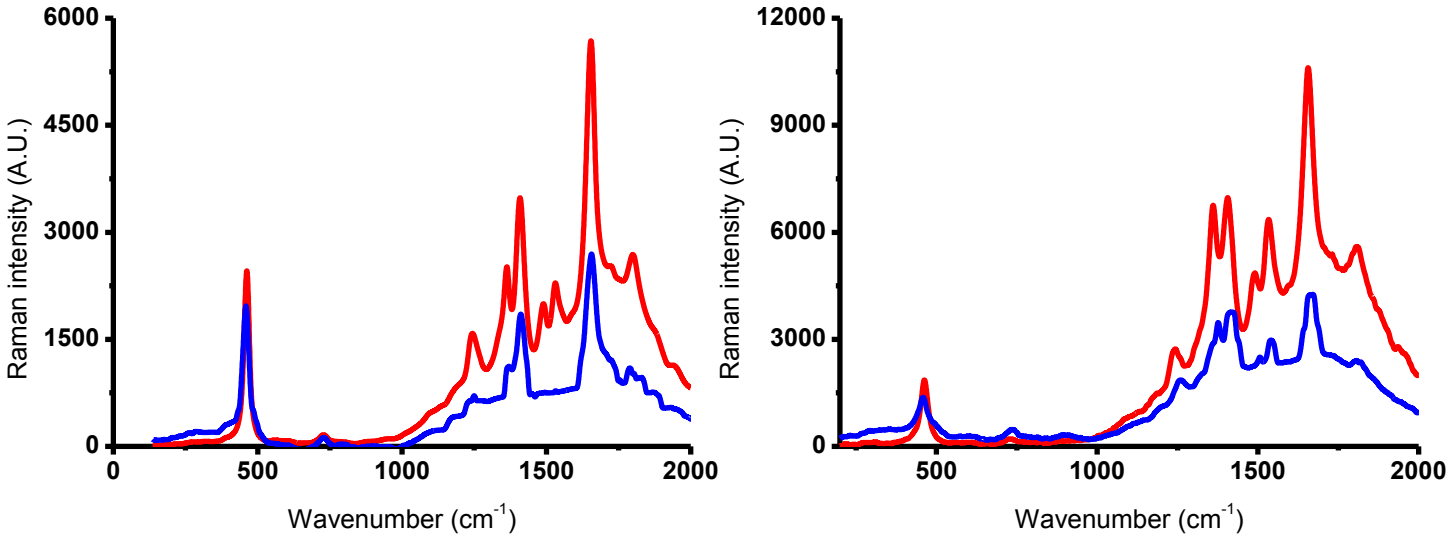

(a) (b)

Figure 5. Raman Spectra of CeO_2 (a) and $Ce_{0.8}Zr_{0.2}O_2$ (b) in the presence (lower plots) and absence (upper plots) of Printex U. The spectra in the presence of soot have been increased by factors of 5 and 20 respectively.

Figure 6

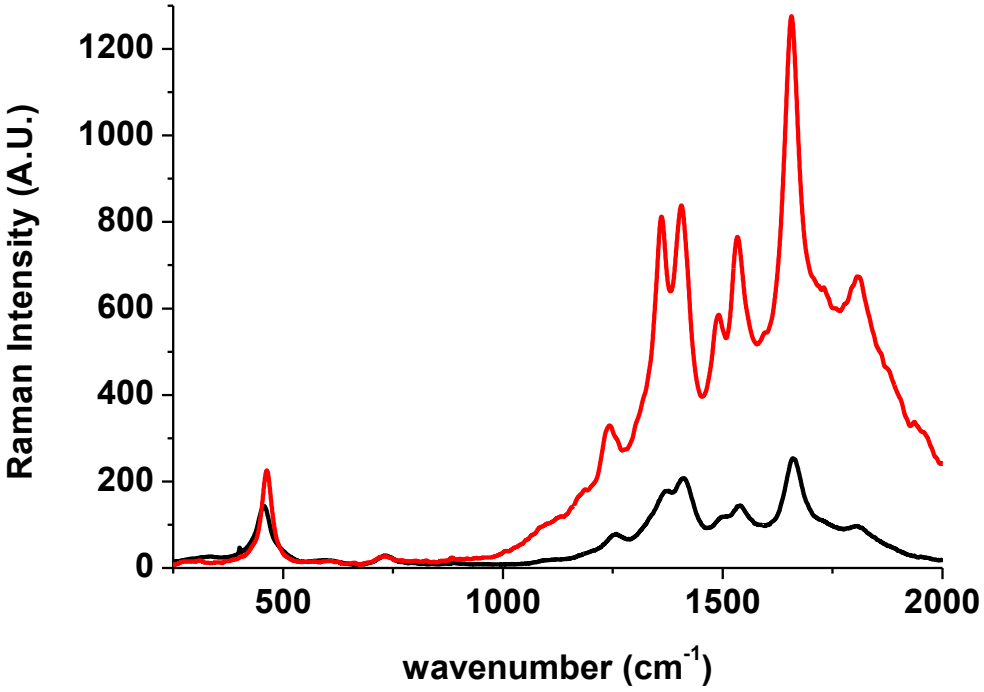

Figure 6. Raman spectra of a $Ce_{0.8}Zr_{0.2}O_2$ catalyst soot mixture before (lower profile) and after (upper profile) a treatment in NO / O_2 at 500 °C. Spectra were recorded at room temperature

Figure 7

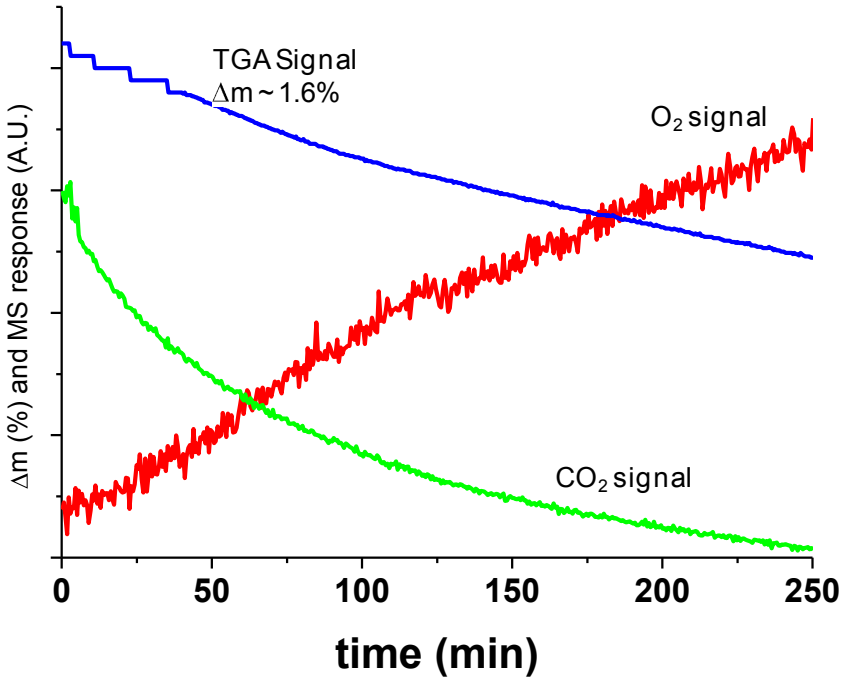

a

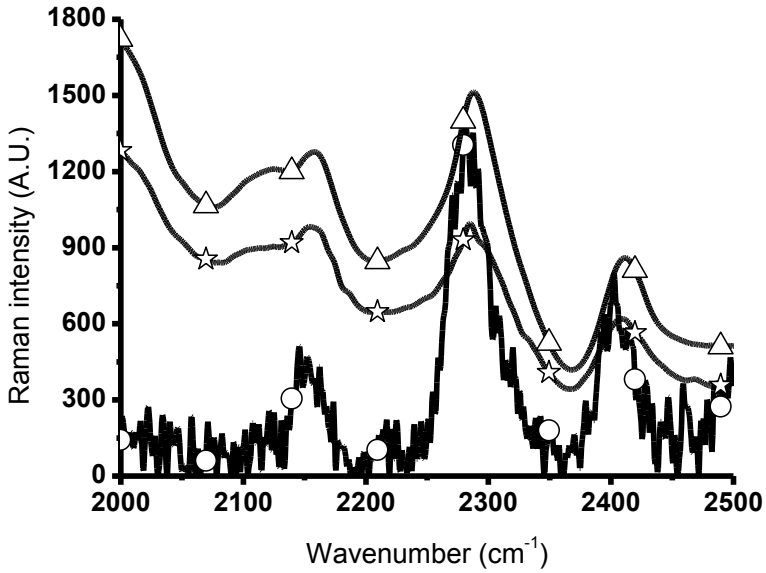

b

Figure 7 (a) TGA and evolved O_2 and CO_2 profiles recorded during an experiment where a $Ce_{0.8}Zr_{0.2}O_2$ – PM mixture was subjected to a flow of He at 500 °C.

Figure 7(b) Normalised Raman spectra of a fresh sample of CeZ20 - U fresh (○), and exposed to an inert atmosphere at 500 °C for 4 hours (☆) for 30 hours (△).

Supplementary Information for

An *in-situ* Raman study of Ceria/Zirconia catalysts in PM combustion

James A Sullivan,[1] Petrica Dulgheru[1,3], Idriss Atribak[2], Agustín Bueno- López[2], Avelina García-García,[2]

Figure S1

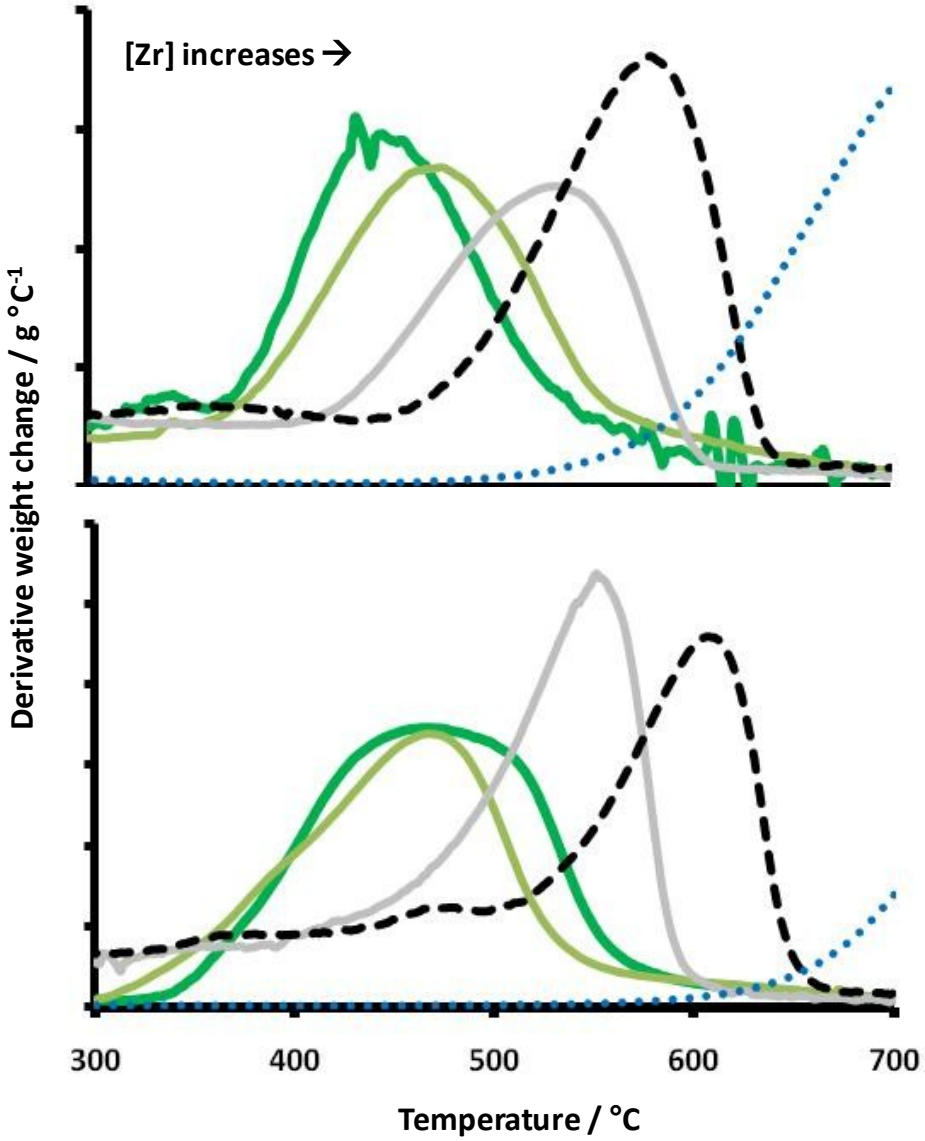

Figure S1 Activity of a selection of the different solid solutions in promoting soot combustion in Air (lower plots) and NO/O_2 (upper plots) as measured using TGA. Activity in each case is proportional to [Ce] in the catalyst. The non-catalysed combustion is shown in each case as a dotted line.

Figure S2

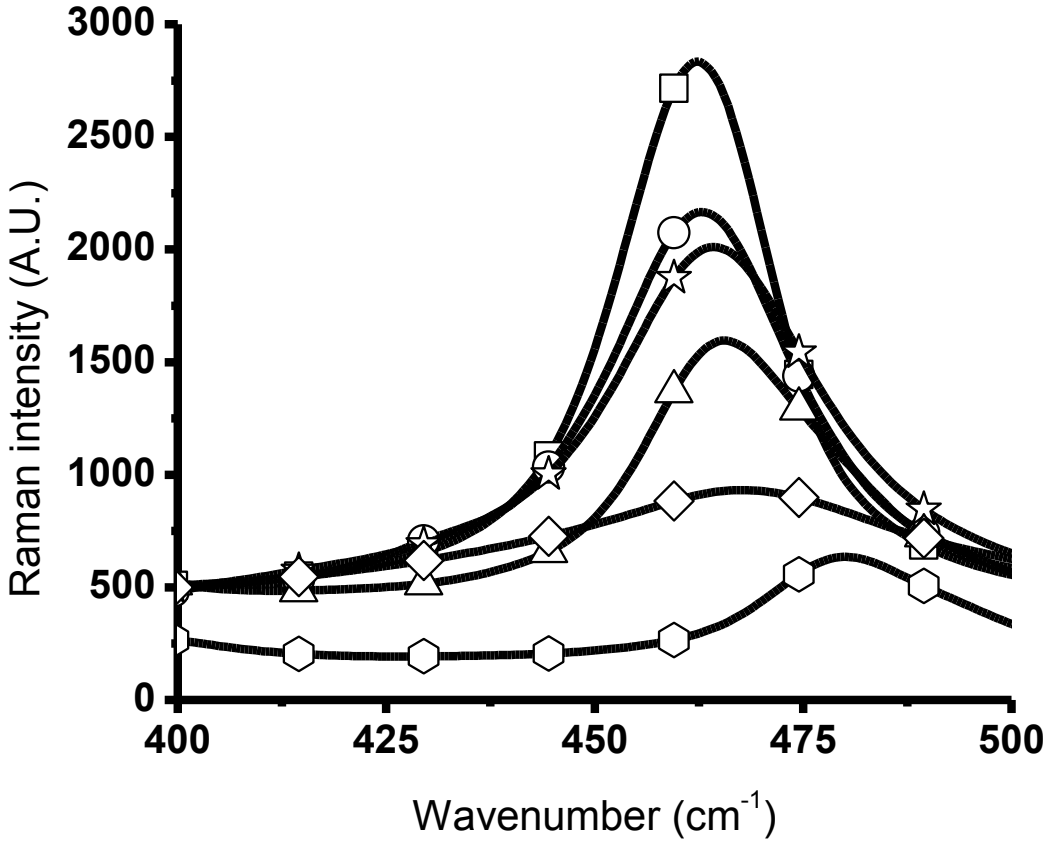

Figure S2. Room temperature Raman spectra showing the variation in the F_{2g} peak as [Zr] in the solid solution changes. CeO_2,(□), $Ce_{0.8}Zr_{0.2}O_2$ (○),$Ce_{0.6}Zr_{0.4}O_2$ (◇),$Ce_{0.4}Zr_{0.6}O_2$ (☆), $Ce_{0.2}Zr_{0.8}O_2$ (△) and ZrO_2 (■)

Figure S3

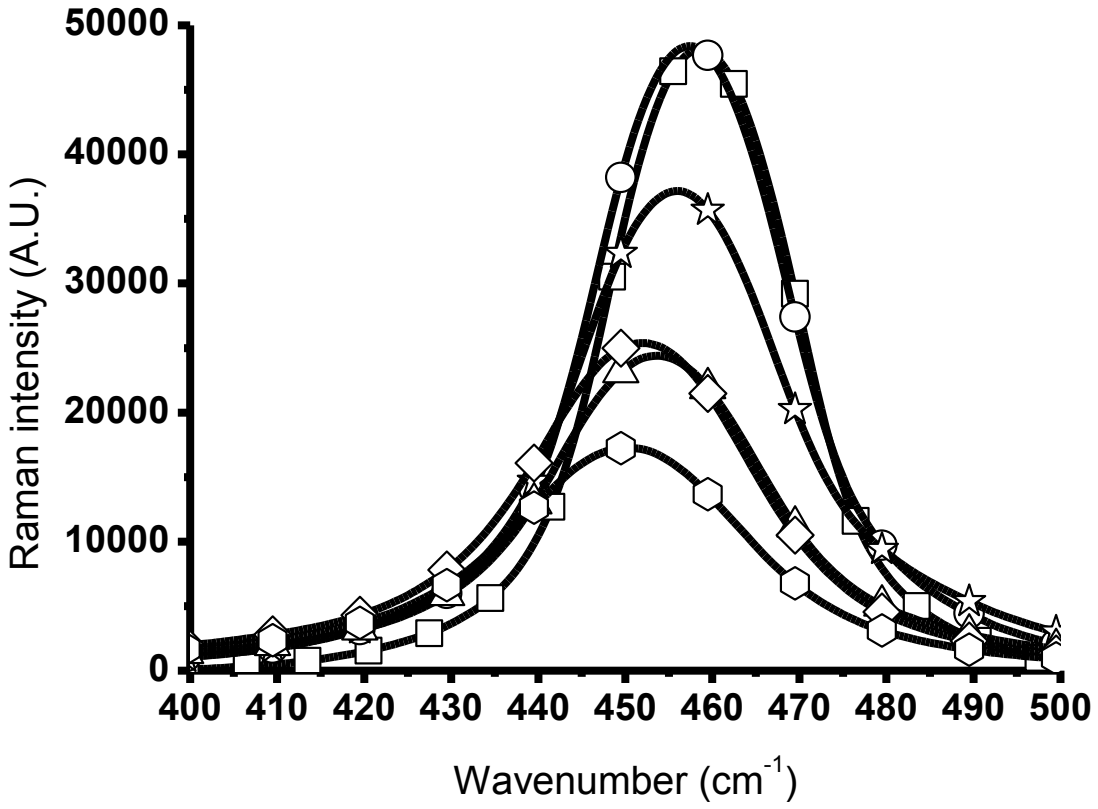

Figure S3. Showing 400 - 500 cm^{-1} region of the Raman spectra of CeO_2 recorded at: RT (□), 100 °C (○), 200 °C (☆), 300 °C (△) 400 °C (◇), and 500 °C (■) while being exposed to 10 mL min^{-1} H_2.

Figure S4

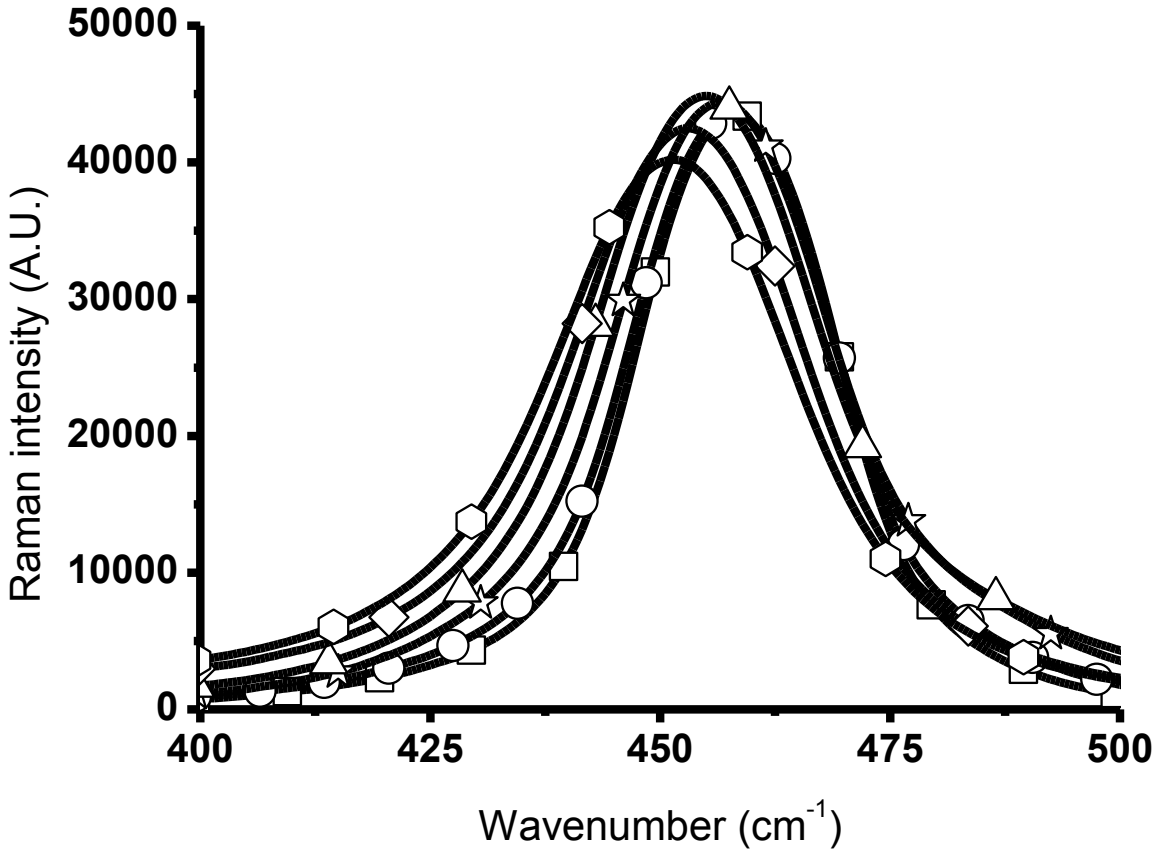

Figure S4. Showing 400 - 500 cm^{-1} region of the Raman spectra of CeO_2 recorded at: RT (□), 100 °C (○), 200 °C (☆), 300 °C (△) 400 °C (◇), and 500 °C (■) while being exposed to 10 mL min^{-1} O_2.

Figure S5

Under the spectral collection conditions used on our work samples containing higher concentrations of Zr fluoresce (see figure S5 (a) and 3(c)). A certain amount of this fluorescence can be corrected using concave rubber band correction (see figure S5(b)). However, at the highest loadings of Zr within the lattices concave rubber band correction is no longer effective (see figure S5(d)).

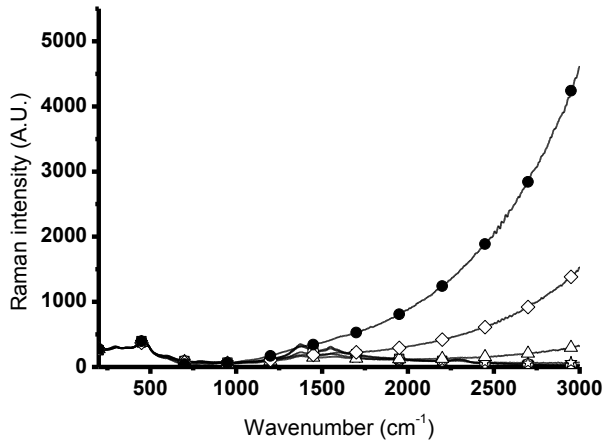

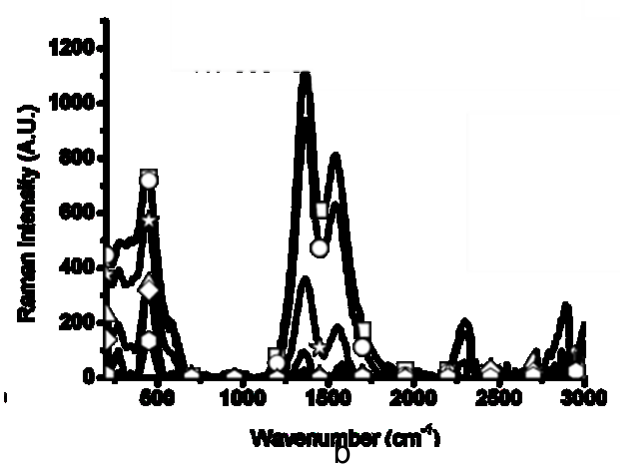

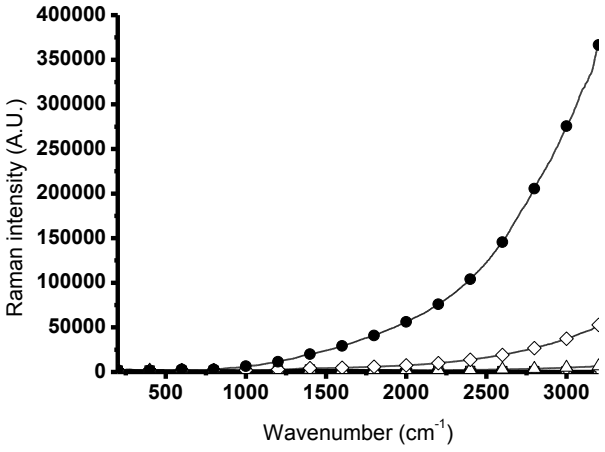

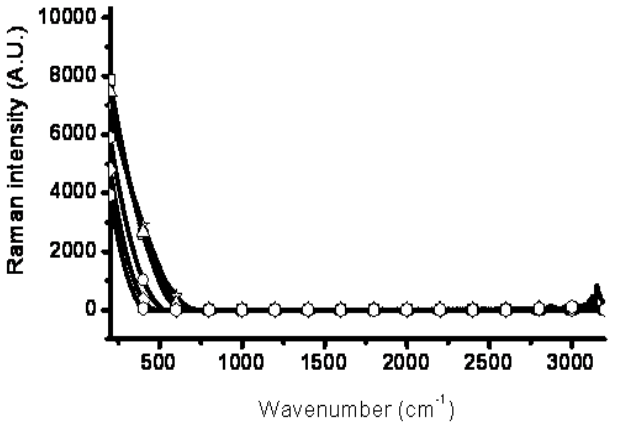

Figure S5. Raman Spectra recorded during exposure of $Ce_{0.4}Zr_{0.6}O_2$–PM mixtures (plots (a) and (b)) and $Ce_{0.2}Zr_{0.8}O_2$–PM mixtures (plots (c) and (d)) to NO/O_2 between RT and 500 °C. RT (□), 100 °C (○), 200 °C (☆), 300 °C (△), 400 °C (◇), 500 °C (●). Plots (a) and (c) show the raw spectra while plots (b) and (d) show the effect of concave rubber band correction on the spectra.

Figure S6

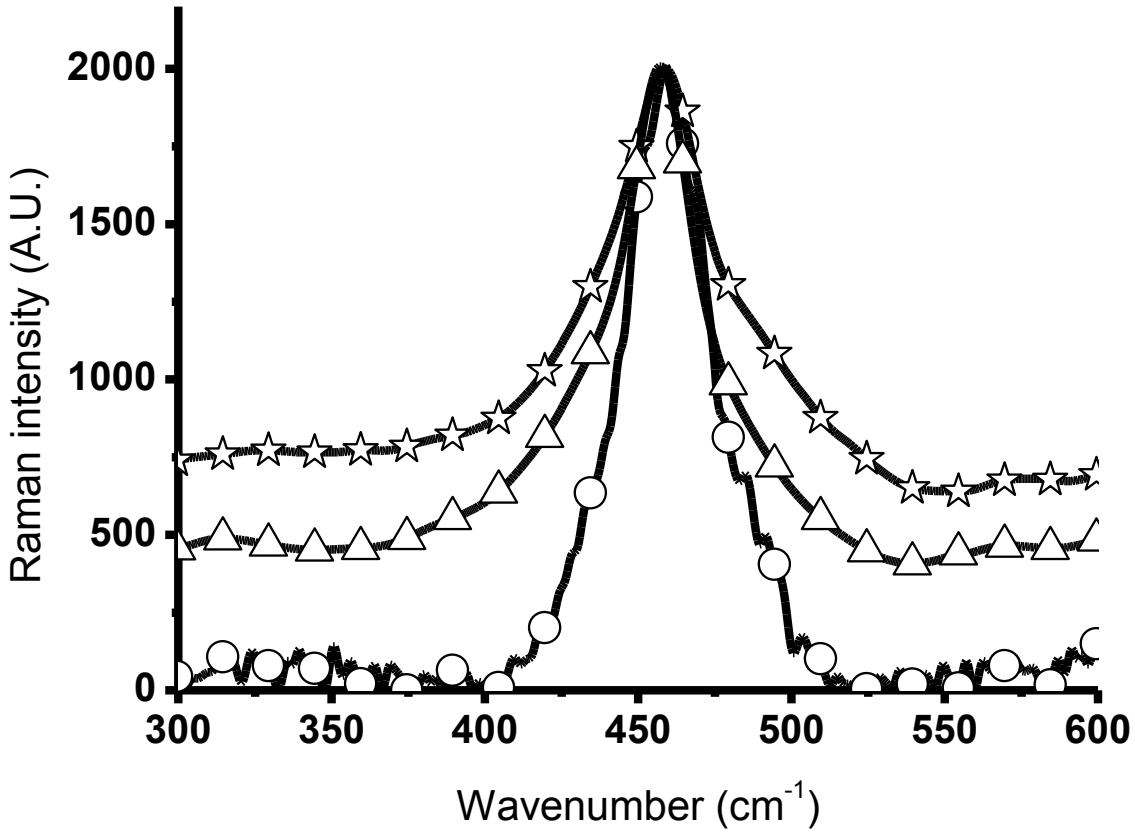

Figure S6. Normalised F_{2g} region of the Raman spectra of a $Ce_{0.8}Zr_{0.2}O_2$ sample following the treatments shown in Figure 7. Fresh $Ce_{0.8}Zr_{0.2}O_2$ - PM (○), $Ce_{0.8}Zr_{0.2}O_2$ - PM exposed to an inert atmosphere for 4 hours at 500 °C (☆) and $Ce_{0.8}Zr_{0.2}O_2$ - PM exposed to an inert atmosphere for 30 hours at 500 °C (△).